Abstract

Purpose: The Photopic Negative Response is a component of the light-adapted electroretinogram (ERG) that is reduced in glaucomatous eyes and the Bruch's Membrane Opening - Minimum Rim Width (MRW) than Retinal Nerve Fiber Layer (RNFL) thickness are two structural measures of retinal ganglion cell related structures that are disrupted in glaucomatous eyes. The purpose of our investigation was to determine whether the PhNR amplitude in primary open angle glaucoma patients is better correlated with Bruch's Membrane Opening - Minimum Rim Width (MRW) than Retinal Nerve Fiber Layer (RNFL) thickness.

Methods: Full-field Photopic Flash ERGs to brief red flashes delivered on a rod-saturating blue background were recorded from one eye of glaucoma patients (N=10) and age-matched controls (N=10) using an electrophysiological system from Diagnosys (Lowell, MA). The PhNR and b-wave responses of the ERG was plotted as a function of test flash strength and fitted with a generalized Naka-Rushton equation to derive values for saturated amplitude, slope and semi-saturation constant. BMO-MRW and peripapillary RNFL thickness were measured from the same eyes using a Spectral-Domain Optical Coherence Tomography system (Spectralis SD-OCT, Heidelberg Inc, Germany). Visual field sensitivity was assessed with the Humphrey Visual Field Analyzer 24-2 SITA standard test (Carl Zeiss Meditec, USA). ERG Naka-Rushton fit parameters were compared between glaucoma patients and age-matched controls. Linear regression analysis was used to study the correlation of significant fit parameters with BMO-MRW, RFNL and average visual field sensitivity.

Results: Of the three different Naka-Rushton fit parameters derived for the PhNR and b-wave only the saturated amplitude of the PhNR was significantly different between

glaucomatous and control subjects (p=0.000002). The PhNR saturated amplitude was significantly correlated only with with BMO-MRW in control eyes (r=0.74, m=0.1, p=0.0002) and in glaucomatous eyes showed a better correlation with BMO-MRW (r=0.91, m=0.05, p=0.0002) than with RNFL thickness (r=0.7, m=0.18, p=0.03). PhNR saturated amplitude was also correlated with average behavioral visual sensitivity in glaucomatous eyes (r=0.72, m=29.9, p=0.02).

Conclusion: The variance in PhNR amplitude in control and glaucomatous eyes is better accounted for by BMO-MRW than RNFL thickness. This finding may reflect an optic nerve head and prelaminar optic nerve being the locus of PhNR generation as well as early pathogenic events in glaucoma.

Introduction

Glaucoma is a disease characterized by progressive vision loss that is secondary to retinal ganglion cell dysfunction and death [1]. The photopic negative response (PhNR), a slow electrical potential of negative polarity in the full-field flash electroretinogram (ERG) is generated by inner retinal neurons, primarily the retinal ganglion cells [2], providing a non-invasive and objective evaluation of retinal ganglion cell function in glaucomatous eyes [3-15]. However, the correlation between PhNR amplitude and retinal nerve fiber layer (RNFL) thickness as measured with the Ocular Coherence Tomography (OCT) technique is, at best, only moderate [16-19]. The RNFL thickness measurement with the OCT is typically performed as a circular scan of fixed diameters of 3.5, 4.1 or 4.6 mm centered around the optic disc. Mechanical compression of the prelaminar optic nerve and the nerve head is generally considered the primary pathogenetic event in glaucomatous damage [20]. Thus exploring comparisons of parameters of optic nerve head structure with retinal ganglion cell function could provide insights into the structural underpinnings of progressive retinal ganglion cell dysfunction and visual deterioration in glaucoma. Recent advances in optic nerve head imaging with the OCT have identified a novel way to characterize the neuroretinal rim width, a measure that is termed the Bruch's Membrane Opening (BMO) - Minimum Rim Width (MRW) obtained by measuring the minimum distance from the outer border of the BMO to the internal limiting membrane (ILM). This has been suggested to have better diagnostic accuracy than RNFL thickness for the detection of glaucomatous damage and providing better correlations with functional deficits [21-24]. The purpose of our investigation was to determine whether the PhNR amplitude in primary open angle glaucoma patients is better correlated with BMO-MRW than RNFL thickness.

Methods

Ten patients with a diagnosis of primary open angle glaucoma (POAG) in the age range of 54-76 years (mean age 63.5±8 years) comprising 5 males and 5 females with different degrees of severity were recruited from the University Eye Center (UEC) at State University of New York College of Optometry. The inclusion criteria included a mandatory clinical diagnosis of POAG by experienced clinical practitioners using a battery of clinical tests, which included a detailed case history, indirect ophthalmoscopy, applanation tonometry, visual field testing, visual field trend analysis, posterior segment photography and optical coherence tomography. Patients with any history of other ocular disease (except uncomplicated cataract) or systemic conditions that could affect the study outcomes were excluded. The patients had best-corrected visual acuity of 20/30 or better and their refractive error was within ± 6D spherical equivalent. The inclusion criteria for a diagnosis of glaucoma was based upon the presence of glaucomatous optic neuropathy and characteristic visual field loss associated with glaucoma (e.g., hemifield test outside normal limits, a cluster of three contiguous points at the 5% level of the pattern deviation plot). The vertical dimension of the cup to disc ratio also proved to be an index of the glaucomatous loss to the neuroretinal rim. All the patients were under medical treatment for control of their intraocular pressure. Similarly, 10 healthy, visually normal subjects without POAG in the age range of 53 to 74 years (mean age 66.1±7.5 years) comprising 5 males and 5 females were also enrolled. The difference in ages between the two groups was not statistically significant ($p=0.46$). Subject demographics, mean deviation of 24-2 Visual Field sensitivity (in dB), Bruch's Membrane Opening - Minimum Rim Width (in microns) and average retinal nerve fiber layer thickness (in µm) are summarized in Table 1. Written consent was obtained from all the participants and the study strictly adhered to

the declaration of Helsinki and was approved by the Institutional Review Board at the State University of New York College of Optometry.

Only one eye was tested for each participant. Following the installation of one drop of topical anesthesia (1% Proparacaine Hydrochloride, Akorn, Lake Forest, Illinois, USA), DTL electrodes (Diagnosys LLC, Lowell, MA, USA) were placed in the lower cul-de-sac of the tested eye and referenced to another electrode in the fellow eye that was covered with a light proof patch. An ear clip electrode on the earlobe on the side of the tested eye served as ground. For glaucoma patients, the active electrode was always placed on the eye with the greater magnitude of glaucomatous field defect when possible, whereas the right eye was always tested for the control subjects.

Pupils were dilated to at least 7 mm with the application of 1% topical Tropicamide (Akorn, Lake Forest, Illinois, USA) and the subjects were adapted to the background light for 10 minutes prior to start of the test. Visual stimulation and response acquisition were performed with an Espion system from Diagnosys LLC. A series of red flashes (660 nm peak λ) ranging from 0.00625 to 6.4 phot cd.s/m^2 were delivered on a steady blue background (485 nm peak λ) of 7 phot cd/m^2 using the Colordome ganzfeld (Diagnosys LLC, Lowell, MA, USA). Approximately 25 responses were averaged for each flash intensity, with an interstimulus interval of at least 1 second. An infrared camera inside the ganzfeld was used to monitor eye fixation and traces contaminated with blinks and eye movements were excluded from the analysis. Signals were sampled at 1 kHz, amplified, filtered within the range of 0 to 300 Hz, and digitized.

The PhNR was measured from baseline to the PhNR trough following the i-wave. At flash intensities where the PhNR trough was not prominent, the amplitudes were

measured at times when the trough was the most prominent in the succeeding brighter flash. (this sentence needs clarification). The b-wave amplitude was measured at its peak from the preceding a-wave trough.

The PhNR and b wave amplitudes were plotted as a function of stimulus strength and fit with a generalized Naka-Rushton equation of the form $V(I) = (V_{max}*I^n)/(I^n+K^n)$: where I is the stimulus intensity; V is the amplitude at intensity I; V_{max} is the saturated amplitude; K is the semi-saturation constant or the intensity at which the amplitude is half of V_{max}, and n is the slope. SigmaPlot (Version 10, Systat Software, Inc., San Jose, CA) was used for curve fitting and all subsequent statistical analysis. The slopes of the individual fits were not constrained to any value and the fits were achieved by minimizing the sum of the squared differences between the observed and predicted data.

Behavioral visual field sensitivity was assessed with the Humphrey Visual Field Analyzer (Carl Zeiss Meditec, USA) using the 24-2 SITA standard test. A visual field was considered reliable when the fixation losses were <20% and false negative as well as false positive rates were under 25%. The dB values at each test location were converted to linear values and averaged across the entire visual field to derive mean sensitivity values on a linear scale.

Figures 1 and 2 illustrate the OCT measures of the BMO-MRW and RNFL. Spectral-domain optical coherence tomography (Spectralis SD-OCT, Heidelberg Inc, Germany) scans of the optic nerve head and peripapillary retinal nerve fiber layer were performed. To assess the neuroretinal rim width, 24 radially equidistant OCT scans centered on the optic nerve head were captured. For each radial scan, the algorithm computed the shortest distance between the BMO and ILM and two measures were

derived for each scan from diametrically opposite locations. The average thickness of the neuroretinal rim was then calculated by combining the measurements from the 24 scans. BMO-centered OCT scans also give the peripapillary retinal nerve fiber layer (pRNFL) thickness at three eccentricities (3.5mm, 4.1mm, and 4.7mm), but only the thickness measures from the 3.5mm diameter scan were used for analysis. The machine algorithm, which determined the inner and outer boundary of the retinal nerve fiber layer thickness, also provided an estimate of the average thickness. For both the BMO-MRW and RNFL thickness measurements, manual corrections were made to the segmentation profiles generated by the algorithm to correct any small aberrations.

Statistical analysis was performed with unpaired student t tests to compare the mean differences of the Naka-Rushton fit parameters between glaucoma patients and age-matched controls. The association between the Naka-Rushton fit parameters and RNFL thickness, BMO-MRW, and mean visual field sensitivity were studied by using simple linear regressions. A p-value less than 0.05 was considered as significant after correcting it for multiple comparisons using Holm's method of correction [25].

Results

Figures 3A and B illustrate representative photopic ERG waveforms to increasing test flash strengths from a 55-year-old female control subject and a 51-year-old female glaucoma patient, respectively. These figures capture the general finding from our study that the PhNR amplitude was selectively reduced when the a- and b-wave amplitudes appeared relatively normal. The reduction of the PhNR in the glaucomatous eye also revealed a prominent i-wave in the higher test flash intensity responses. In the control eye responses, the i-wave is seen as a subtle signal in the trailing edge of the b-wave, prior to the PhNR trough. Figures 3C and D illustrate the Naka-Rushton fits to the PhNR intensity response data of the same control subject (solid line and open circles) and glaucoma patient (dashed line and filled circles) for the PhNR and b-wave. Although these figures show the data from selected individuals, they are representative of the general finding that the Naka-Rushton function provides a reasonable description of the intensity response data of all three ERG measures from control subjects as well as glaucoma patients. The amplitudes of the PhNR and b-wave grew with increasing test flash strength, reaching saturation between 0.4 and 1.6 phot cd.s/m^2. The V_{max} for the PhNR of the glaucoma patient illustrated was prominently reduced compared to that of the control subject (19 vs 35μv), while the V_{max} of the b-waves recorded from the glaucoma patient (89 μv) and the control subject (87 μv) were comparable.

The box plots in Figures 4A, B and C illustrate the comparison of V_{max} K and n for the PhNR from control (black) and glaucoma (red) subjects and Figures 4D, E and F illustrates similar comparisons for the b-wave Naka-Rushton fit parameters. In these figures, the thin and thick horizontal lines within the box indicate the median and mean values. The “box” represents the middle 50% of scores for each group. The whiskers

represent the 5th and 95th percentile and the black circles representing the outliers. The mean values of the PhNR V_{max} were significantly different between the glaucoma and control groups (p=0.000002), while the remaining two fit parameters for the PhNR and all three fit parameters for the b-wave were not significantly different.

The box plots in Figures 5A, B and C illustrate comparisons of average RNFL thickness, BMO-MRW and behavioral visual field sensitivity between the control subjects and glaucoma patients. All three measures were significantly different between the two groups (p=0.000005, 0.000004 and 0.00000001 respectively).

Figure 6A illustrates the relationship between PhNR V_{max} and average retinal nerve fiber layer (RNFL) thickness and Figure 6B illustrates the relationship between PhNR V_{max} and average BMO-MRW. In these figures, the black and red circles represent the data from the control and glaucomatous eyes, respectively. Linear regression analysis was used to determine whether the structural measure can predict functional outcome. In control eyes, the PhNR amplitude showed a significant correlation with BMO-MRW (r=0.74, m=0.1, p=0.0002) but not with RNFL thickness (r=0.11, m=0.05, p=0.74). In the glaucomatous eyes, while both RNFL and BMO-MRW demonstrated significant correlations with PhNR amplitude, the correlation coefficient was larger for BMO-MRW (r=0.91, m=0.05, p=0.0002) than RNFL thickness (r=0.7, m=0.18, p=0.03). Figure 6C illustrates the relationship between behavioral visual field sensitivity and PhNR V_{max}. In control eyes, on visual inspection the visual field sensitivity demonstrated a tendency to reduce with the magnitude of PhNR amplitude, however this trend was not statistical significance (r=0.56, m=14.1, p=0.09). However, a similar trend observed in glaucomatous eyes demonstrated statistical significance (r=0.72, m=29.9, p=0.02).

Discussion

From linear regression analysis, we not only found that the proportion of the variance in PhNR V_{max} was better accounted by the BMO-MRW than RNFL thickness (81% vs 49%) in glaucomatous eyes but also that 55% of the variance in the PhNR V_{max} in the control eyes could be accounted for by BMO-MRW. RNFL thickness could hardly account for any of the PhNR V_{max} variance in control eyes. To the best of our knowledge these findings have not been previously reported.

The retinal locus and cellular mechanisms that generate the PhNR, together with the nature of early damage to the optic nerve head in glaucoma, can perhaps explain our findings. While the PhNR clearly relies on the spiking activity of retinal ganglion cells [2], the nature of its slow time course and reduction by suppression of K^+ currents in glial cells [26] suggest glial mediation in its generation. The convergence of the retinal nerve fibers at the optic nerve head, which are unmyelinated in the prelaminar optic nerve, positions this location as a site of a large increase of extracellular K^+ during the propagation of action potentials. Further, the high density of astrocytes in the optic nerve head [27-28] along with their parallel organization in the prelaminar optic nerve connected linearly and laterally with surrounding astrocytes via gap junctions [29] serves to siphon the K^+ released by the ganglion cell axons, perhaps via Kir6.1 channels [30] to direct them towards the vitreous. These glial cell related radial extracellular current loops are likely involved in mediating the PhNR recorded at the level of the cornea. Thus, the cellular elements that are crucial to the generation of the PhNR and their retinal locus can explain why the variance in PhNR amplitude in control eyes is better correlated to BMO-MRW than RNFL thickness.

Mechanical compression of the prelaminar optic nerve and the nerve head is generally considered the primary pathogenetic event in glaucomatous damage [20].

Clinically, while glaucoma is described as a condition characterized by retinal ganglion cell dysfunction and death, a growing body of evidence suggest that glial transformations manifest early in the disease process before significant neuronal changes by some accounts [31-35]. Consequently, changes in glial cell numbers and/or connectivity in the early stages of the disease can conceivably disrupt the K^+ currents within the optic nerve head astrocytes and reduce the PhNR amplitude prior to neuronal degeneration. Further, glial changes in the optic nerve head are likely to be reflected earlier in structural measures like the BMO-MRW, which are performed at the optic nerve head, rather than peripapillary RNFL thickness. This can also explain why PhNR amplitude is better correlated with and BMO-MRW than RNFL thickness. Likewise, this can also explain the significant correlation between behaviorally measured visual sensitivity and PhNR amplitude in this study.

In conclusion, our results indicate that the PhNR amplitude is better correlated with BMO-MRW than with RNFL thickness measurement in glaucomatous and control eyes. The PhNR thus holds promise for early detection of functional disruption in glaucomatous eyes. Longitudinal studies are needed to determine whether PhNR changes can be detected in pre-perimetric eyes and can then be used as a predictor of disease progression.

Subject ID	Gender	Age (yrs)	VFS(1/L)	Avg. RNFLT (µm)	BMO-MRW (µm)
C1	M	53	979	113	342
C2	F	54	977	128	403
C3	M	55	575	103	290
C4	F	59	783	123	343
C5	M	65	793	126	312
C6	F	72	914	107	319
C7	F	63	862	127	400
C8	M	68	695	105	380
C9	M	72	838	101	347
C10	F	74	760	117	360
G1	M	67	190	96	251
G2	F	75	239	86	214
G3	M	76	25	54	107
G4	M	63	33	85	181
G5	M	69	364	93	304
G6	F	68	179	58	147
G7	F	72	213	75	213
G8	F	54	441	86	200
G9	M	57	466	85	260
G10	F	60	298	69	133

Table 1: Shows basic demographic information of the control subjects (C1-C10) and glaucoma patients (G1-G10) along with their gender, age, average visual field (VFS) in linear units (1/Lamberts) from 24-2, average retinal nerve fiber layer thickness (RNFLT) in microns and Bruch's membrane Opening – Minimum Rim Width (BMO-MRW) in microns.

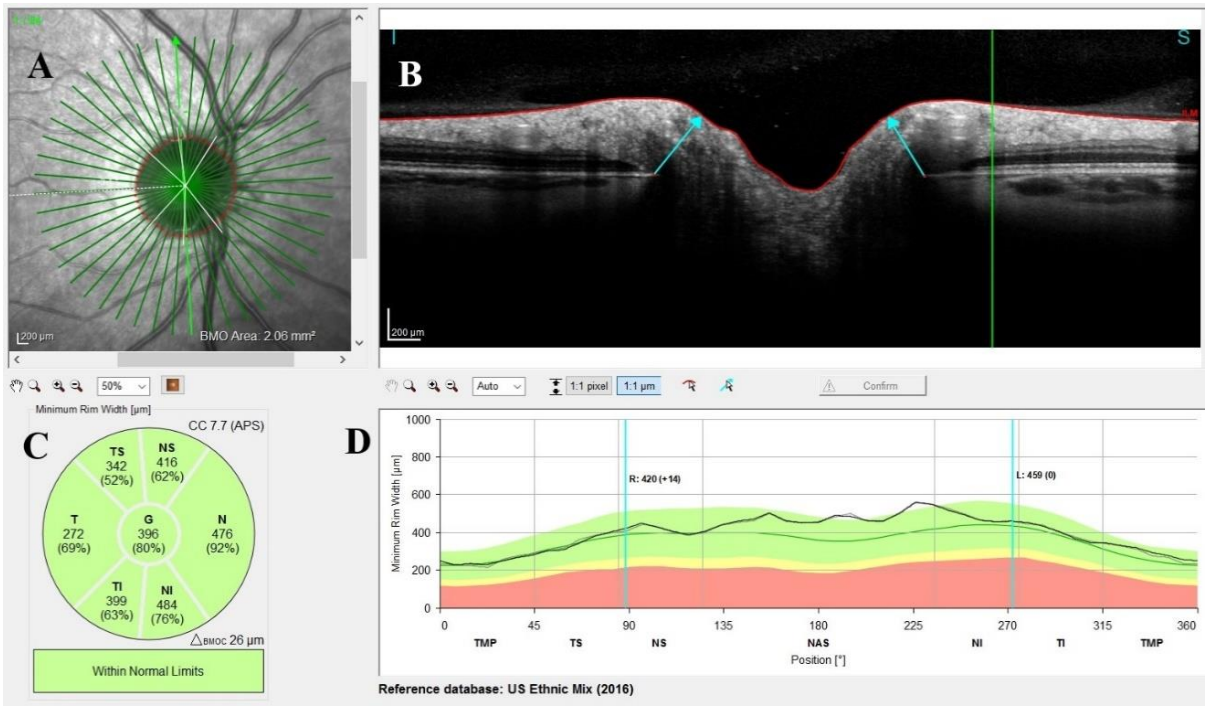

Figure 1: Bruch's Membrane Opening – Minimum Rim Width (BMO-MRW) for a control subject (**A**) Meridians of 24 radial scans (**B)** Arrows marking the minimal distance from the BMO to the inner limiting membrane (C) Average BMO-MRW for different sectors (**C**), and thickness profiles (**D**) BMO-MRW across 360 degrees.

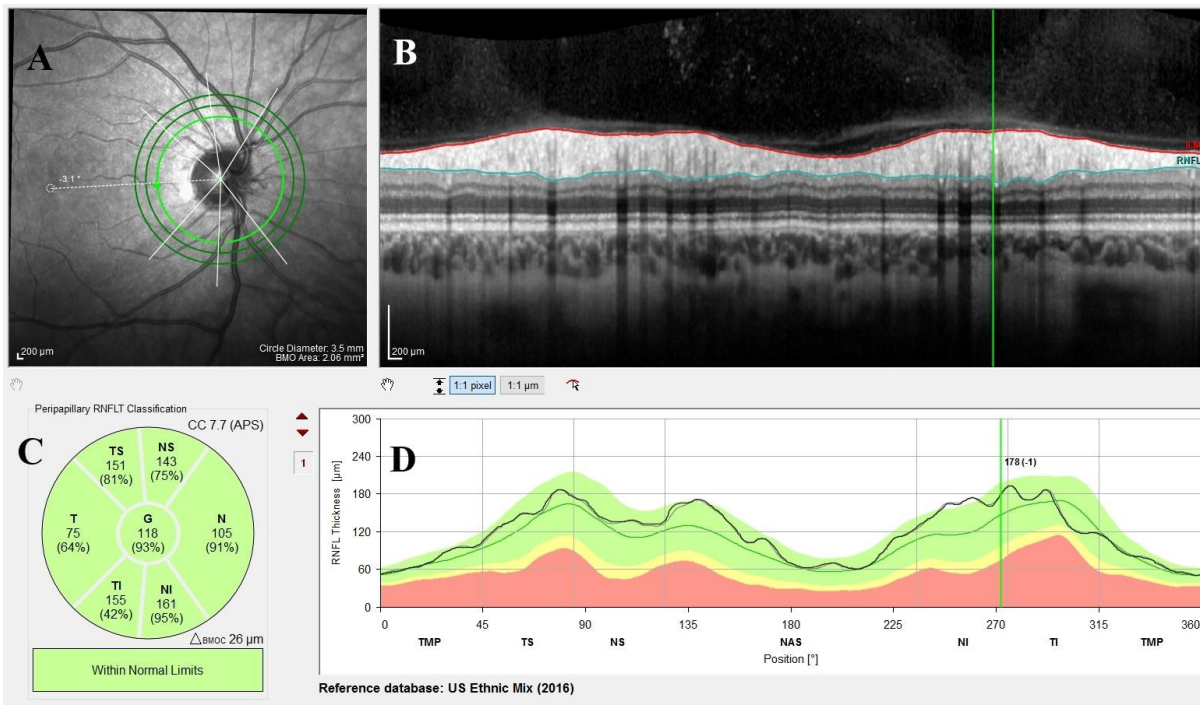

Figure 2: Peripapillary retinal nerve fiber layer (pRNFL) thickness for a control subject (**A**) 3.5 mm diameter ring centered on the optic disc **(B)** The temporal-superior nasal-inferior- temporal (TSNIT) thickness profile (**C**) The average pRNFL thickness for different sectors (**D**) Thickness profile across 360 degrees.

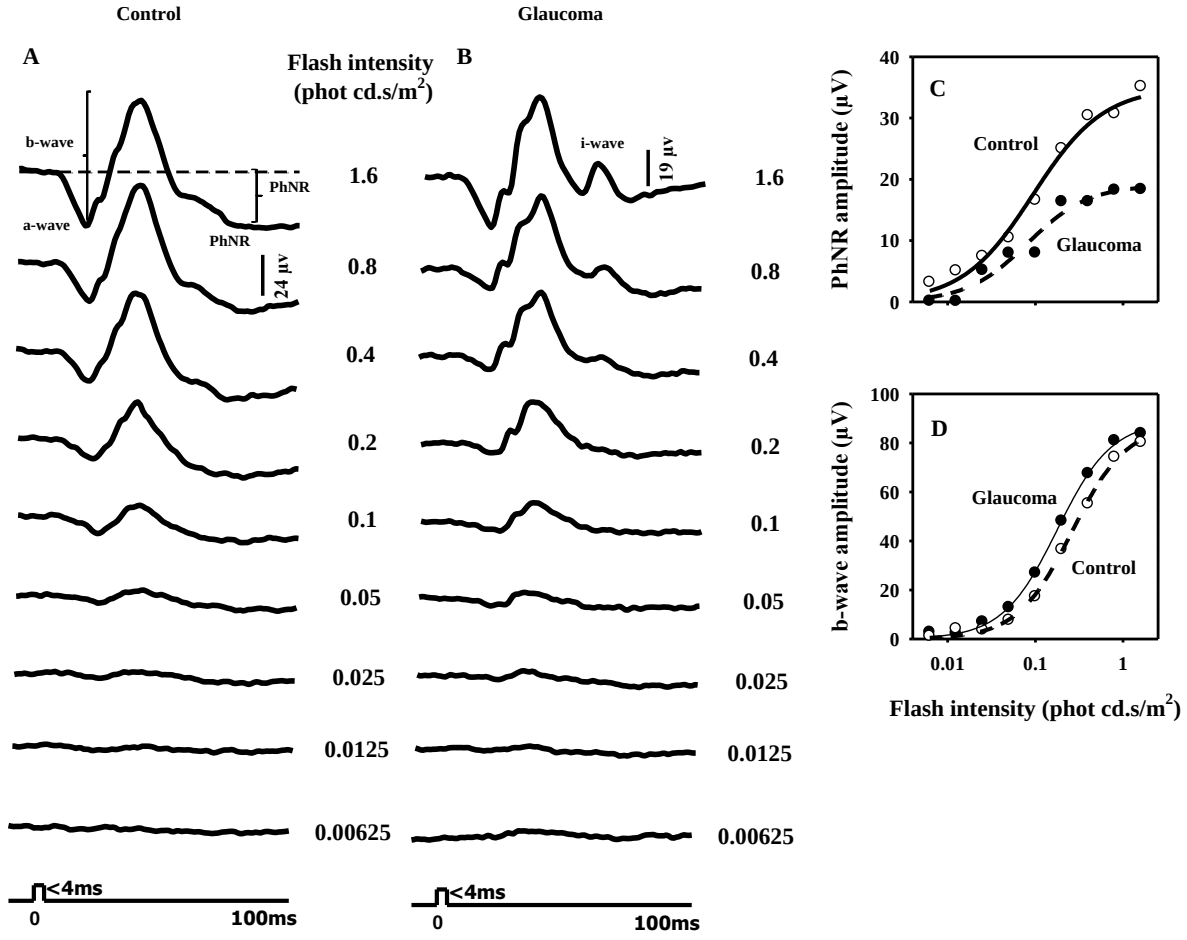

Figure 3: Examples of photopic ERG waveforms to increasing test flashes from a 55-year old female control subject (A) and a 51-year-old glaucoma patient (B) with illustration of a wave, b wave and PhNR as well as the Naka-Rushton fits to the intensity response data for the PhNR (C), (D) respectively.

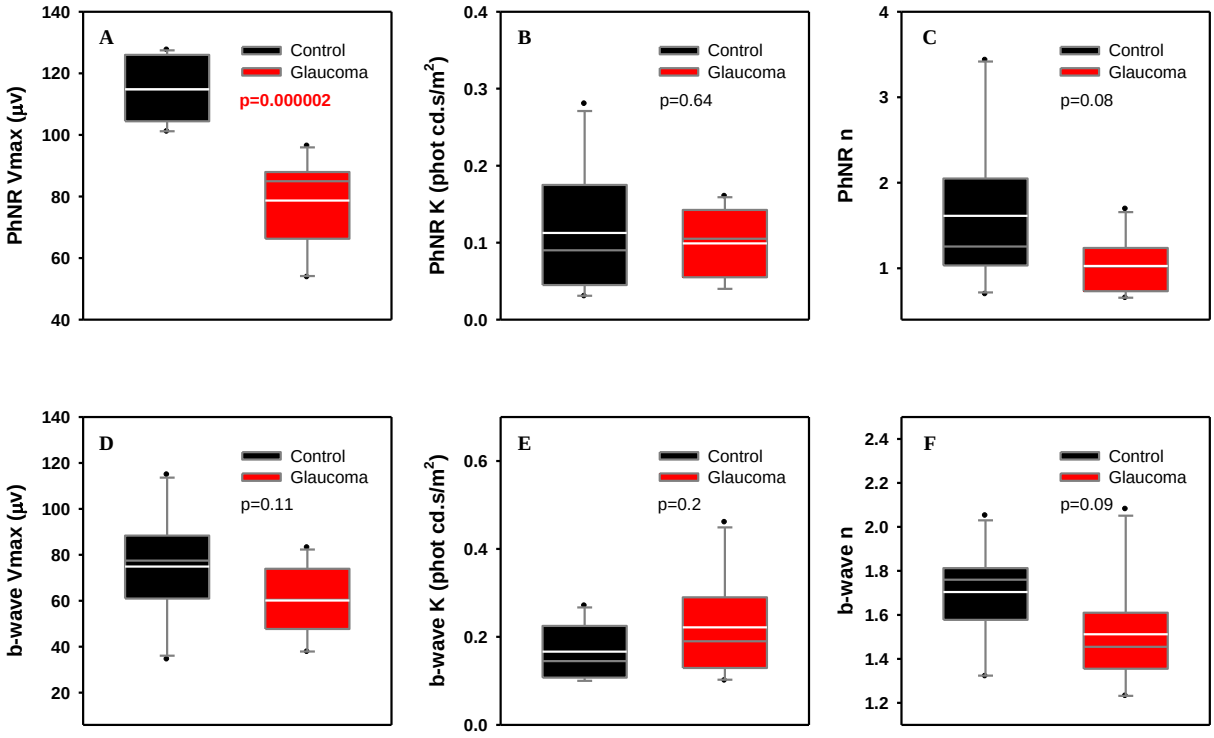

Figure 4: Box plots for control (black) and glaucoma (red) cohorts illustrating the distribution of Naka-Rushton fit parameters for PhNR: Vmax (A), K (B) and n (C) and b-wave Vmax (D), K (E) and n (F). The thin and thick horizontal lines within each box indicate the median and mean values. The box represents the middle 50% of values and the whiskers represent the 5th and 95th percentile with the black circles representing the outliers.

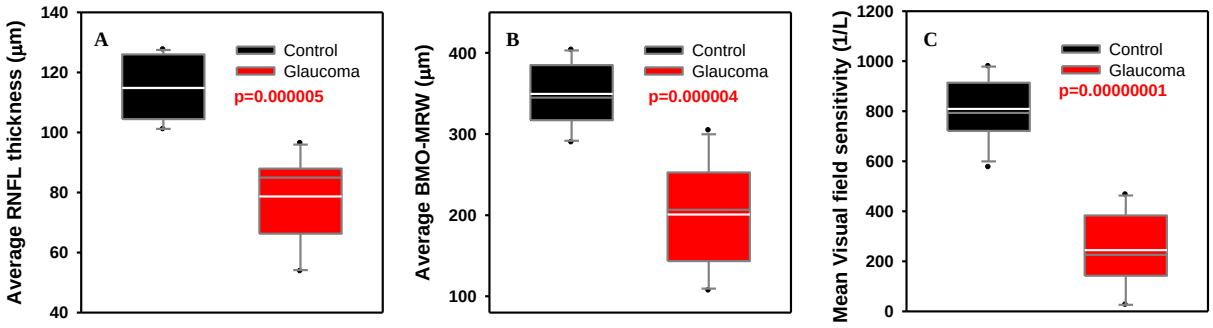

Figure 5: Box plots for control (black) and glaucoma (red) cohorts illustrating the distribution of average RNFL thickness (A), BMO-MRW (B) and behavioral visual field sensitivity (C). The thin and thick horizontal lines within each box indicate the median and mean values. The box represents the middle 50% of values and the whiskers represent the 5th and 95th percentile with the black circles representing the outliers.

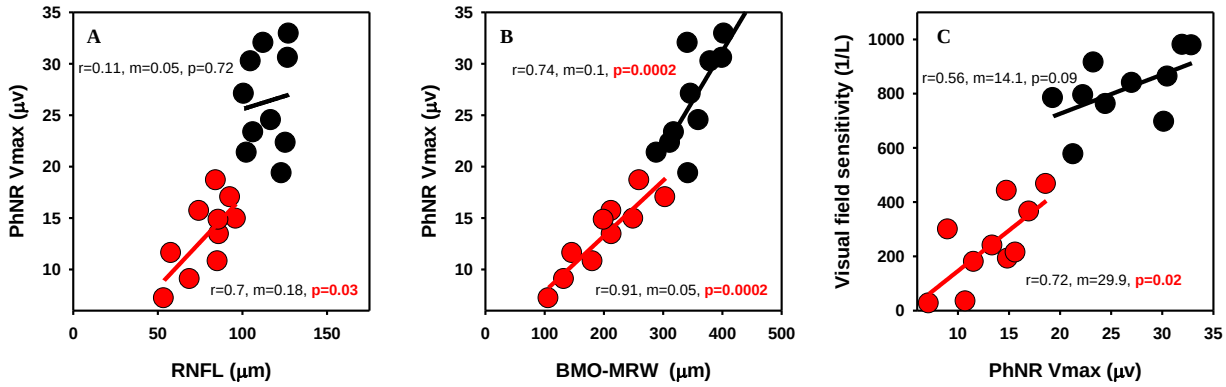

Figure 6: Illustrates linear regression analysis or relationship between (A) PhNR Vmax and RNFL (B) PhNR Vmax and BMO-MRW and (C) Average visual field sensitivity and PhNR Vmax.

References

1. Casson RJ, Chidlow G, Wood JP, Crowston JG, Goldberg I. Definition of glaucoma: clinical and experimental concepts. Clinical & experimental ophthalmology. 2012 May 1;40(4):341-9.
2. Viswanathan S, Frishman LJ, Robson JG, Harwerth RS, Smith EL 3rd. (1999) The photopic negative response of the macaque electroretinogram: reduction by experimental glaucoma. Invest Ophthalmol Vis Sci 40:1124-1136
3. Viswanathan S, Frishman LJ, Robson JG, Walters JW. (2001) The photopic negative response of the flash electroretinogram in primary open angle glaucoma. Invest Ophthalmol Vis Sci 42:514-522
4. Drasdo N, Aldebasi YH, Chiti Z, Mortlock KE, Morgan JE, North RV. (2001) The s-cone PHNR and pattern ERG in primary open angle glaucoma. Invest Ophthalmol Vis Sci 42:1266-1272
5. Wu Z, Hadoux X, Fan Gaskin JC, Sarossy MG, Crowston JG (2016) Measuring the Photopic Negative Response: Viability of Skin Electrodes and Variability Across Disease Severities in Glaucoma. Transl Vis Sci Technol 5:13
6. Machida S, Gotoh Y, Toba Y, Ohtaki A, Kaneko M, Kurosaka D. (2008) Correlation between photopic negative response and retinal nerve fiber layer thickness and optic disc topography in glaucomatous eyes. Invest Ophthalmol Vis Sci 49:2201-2207
7. Sustar M, Cvenkel B, Brecelj J. (2009) The effect of broadband and monochromatic stimuli on the photopic negative response of the electroretinogram in normal subjects and in open-angle glaucoma patients. Doc Ophthalmol. 118:1671-1677

8. North RV, Jones AL, Drasdo N, Wild JM, Morgan JE. (2010) Electrophysiological evidence of early functional damage in glaucoma and ocular hypertension. Invest Ophthalmol Vis Sci 51:1216-1222
9. Horn FK, Gottschalk K, Mardin CY, Pangeni G, Jünemann AG, Kremers J. (2011) On and off responses of the photopic fullfield ERG in normal subjects and glaucoma patients.Doc Ophthalmol 122:53-62
10. Machida S, Tamada K, Oikawa T, Gotoh Y, Nishimura T, Kaneko M, Kurosaka D. (2011) Comparison of photopic negative response of full-field and focal electroretinograms in detecting glaucomatous eyes. J Ophthalmol 2011. Pii: 564131
11. Pangeni G, Lämmer R, Tornow RP, Horn FK, Kremers J. (2012) On- and off-response ERGs elicited by sawtooth stimuli in normal subjects and glaucoma patients. Doc Ophthalmol124:237-248
12. Kremers J, Jertila M, Link B, Pangeni G, Horn FK. (2012) Spectral characteristics of the PhNR in the full-field flash electroretinogram of normals and glaucoma patients. Doc Ophthalmol 124:79-90
13. Niyadurupola N, Luu CD, Nguyen DQ, Geddes K, Tan GX, Wong CC, Tran T, Coote MA, Crowston JG. (2013) Intraocular pressure lowering is associated with an increase in the photopic negative response (PhNR) amplitude in glaucoma and ocular hypertensive eyes. Invest Ophthalmol Vis Sci 54:1913-1919
14. Preiser D, Lagrèze WA, Bach M, Poloschek CM. (2013) Photopic negative response versus pattern electroretinogram in early glaucoma. Invest Ophthalmol Vis Sci 54:1182-1191

15. Kirkiewicz M, Lubiński W, Penkala K. (2016) Photopic negative response of full-field electroretinography in patients with different stages of glaucomatous optic neuropathy. Doc Ophthalmol. 132:57-65
16. Shen X, Huang L, Fan N, He J. (2013) Relationship among Photopic Negative Response,
Retinal Nerve Fiber Layer Thickness, and Visual Field between Normal and POAG
Eyes. ISRN Ophthalmol. 2013 17:182021
17. Banerjee A, Khurana M, Sachidanandam R, Sen P. (2019) Comparison between broadband
and monochromatic photopic negative response in full-field electroretinogram in controls and subjects with primary open-angle glaucoma. Doc Ophthalmol. 138:21-33.
18. Lee J, Kim SA, Lee J, Park CK, Jung KI. (2022) Intereye structure-function relationship using photopic negative response in patients with glaucoma or glaucoma suspect. Sci Rep. 12:13866
19. Tabl AA, Tabl MA. (2022) Correlation between OCT-angiography and photopic negative response in patients with primary open angle glaucoma. Int Ophthalmol. doi: 10.1007/s10792-022-02588-9. Epub ahead of print
20. Quigley HA, Hohman RM, Addicks EM, Massof RW, Green WR. (1983) Morphologic changes in the lamina cribrosa correlated with neural loss in open-angle glaucoma. Am J
Ophthalmol. 95:673-91

21. Chauhan BC, Danthurebandara VM, Sharpe GP, et al. (2015) Bruch's Membrane Opening Minimum Rim Width and Retinal Nerve Fiber Layer Thickness in a Normal White Population: A Multicenter Study. Ophthalmology. 122:1786–1794
22. Danthurebandara VM, Sharpe GP, Hutchison DM, et al. (2014) Enhanced structure-function relationship in glaucoma with an anatomically and geometrically accurate neuroretinal rim measurement. Invest Ophthalmol Vis Sci. 56:98–105
23. Enders P, Adler W, Schaub F, et al. (2016) Novel Bruch's Membrane Opening Minimum Rim Area Equalizes Disc Size Dependency and Offers High Diagnostic Power for Glaucoma. Invest Ophthalmol Vis Sci. 57:6596–6603
24. Torres LA, Sharpe GP, Hutchison DM, et al. (2019) Influence of Bruch's Membrane Opening Area in Diagnosing Glaucoma With Neuroretinal Parameters From Optical Coherence Tomography. Am J Ophthalmol. 208:94–102
25. Holm S. 1979. A simple sequentially rejective multiple test procedure. Scandinavian Journal of Statistics 6:65–70
26. Raz-Prag D, Grimes WN, Fariss RN, et al. (2010) Probing potassium channel function in vivo by intracellular delivery of antibodies in a rat model of retinal neurodegeneration. Proc Natl Acad Sci USA 107:12710-12715
27. Schnitzer J, Karschin A. (1986) The shape and distribution of astrocytes in the retina of the adult rabbit. Cell Tissue Res. 246:91-102.
28. Karschin A, Wässle H, Schnitzer J. (1986) Immunocytochemical studies on astroglia of
the cat retina under normal and pathological conditions. J Comp Neurol. 249:564-76

29. Balaratnasingam C, Kang MH, Yu P, Chan G, Morgan WH, Cringle SJ, Yu DY. (2014)

Comparative quantitative study of astrocytes and capillary distribution in optic nerve laminar regions. Exp Eye Res. 121:11-22

30. Thomzig A, Wenzel M, Karschin C, Eaton MJ, Skatchkov SN, Karschin A, Veh RW.

Kir6.1 is the principal pore-forming subunit of astrocyte but not neuronal plasma membrane K-ATP channels. (2001) Mol Cell Neurosci. 18:671-90.

31. Wang L, Cioffi GA, Cull G, Dong J, Fortune B. (2002) Immunohistologic evidence for retinal glial cell changes in human glaucoma. Invest Ophthalmol Vis Sci 43:1088-1094.

32. Hernandez MR, Miao H, Lukas T. (2008) Astrocytes in glaucomatous optic neuropathy. Prog Brain Res 173:353-73

33. Balaratnasingam C, Morgan WH, Bass L, Ye L, McKnight C, Cringle SJ, Yu DY. (2008) Elevated pressure induced astrocyte damage in the optic nerve. Brain Res. 1244:142-54

34. Son JL, Soto I, Oglesby E, Lopez-Roca T, Pease ME, Quigley HA, Marsh-Armstrong N.(2010) Glaucomatous optic nerve injury involves early astrocyte reactivity and late oligodendrocyte loss. Glia 58:780-789

35. Tehrani S, Johnson EC, Cepurna WO, Morrison JC. (2014) Astrocyte processes label for filamentous actin and reorient early within the optic nerve head in a rat glaucoma model. Invest Ophthalmol Vis Sci 55:6945-52